Clim. Past Discuss., 11, 1407–1435, 2015
www.clim-past-discuss.net/11/1407/2015/
doi:10.5194/cpd-11-1407-2015

Climate of the Past Discussions
Open Access

Millennial-scale precipitation variability over Easter Island (South Pacific) during MIS 3: inter-hemispheric teleconnections with North Atlantic abrupt cold events

O. Margalef[1], I. Cacho[2], S. Pla-Rabes[1], N. Cañellas-Boltà[3], J. J. Pueyo[2], A. Sáez[2], L. D. Pena[2], B. L. Valero-Garcés[4], V. Rull[3], and S. Giralt[3]

[1]Ecological Research Center and Forestry Applications (CREAF), Campus de Bellaterra (UAB) 08193 Cerdanyola del Vallès, Barcelona, Spain
[2]Faculty of Geology, Universitat de Barcelona, Martí Franquès s/n, 08028 Barcelona, Spain
[3]Institute of Earth Sciences Jaume Almera (ICTJA-CSIC), Sedimentary Geology and Geohazards, Lluís Solé i Sabarís s/n, 08028 Barcelona, Spain
[4]Pyrenean Institute of Ecology (IPCSIC), Avda, de Montañana 1005, 50059 Zaragoza, Spain

Received: 13 March 2015 – Accepted: 23 March 2015 – Published: 17 April 2015

Correspondence to: O. Margalef (omargalefgeo@gmail.com)

Published by Copernicus Publications on behalf of the European Geosciences Union.

Abstract

Marine Isotope Stage 3 (MIS 3, 59.4–27.8 kyr BP) is characterized by the occurrence of rapid millennial-scale climate oscillations known as Dansgaard–Oeschger cycles (DO) and by abrupt cooling events in the North Atlantic known as Heinrich events. Although both the timing and dynamics of these events have been broadly explored in North Atlantic records, the response of the tropical and subtropical latitudes to these rapid climatic excursions, particularly in the Southern Hemisphere, still remains unclear. The Rano Aroi peat record (Easter Island, 27° S) provides a unique opportunity to understand atmospheric and oceanic changes in the South Pacific during these DO cycles because of its singular location, which is influenced by the South Pacific Anticyclone (SPA), the Southern Westerlies (SW), and the Intertropical Convergence Zone (ITCZ) linked to the South Pacific Convergence Zone (SPCZ). The Rano Aroi sequence records 6 major events of enhanced precipitation between 38 and 65 kyr BP. These events are compared with other hydrological records from the tropical and subtropical band supporting a coherent regional picture, with the dominance of humid conditions in Southern Hemisphere tropical band during Heinrich Stadials (HS) 5, 5a and 6 and other Stadials while dry conditions prevailed in the Northern tropics. This antiphased hydrological pattern between hemispheres has been attributed to ITCZ migration, which in turn might be associated with an eastward expansion of the SPCZ storm track, leading to an increased intensity of cyclogenic storms reaching Easter Island. Low Pacific Sea Surface Temperature (SST) gradients across the Equator were coincident with the here-defined Rano Aroi humid events and consistent with a reorganization of Southern Pacific atmospheric and oceanic circulation also at higher latitudes during Heinrich and Dansgaard–Oeschger stadials.

CPD
11, 1407–1435, 2015

1 Introduction

With On suborbital timescales, climate in the Northern Hemisphere during MIS 3 was dominated by rapid millennial-scale temperature oscillations defined as the Dansgaard–Oeschger (DO) stadial-interstadial cycles (Dansgaard et al., 1993). During some of the DO stadials, large *armadas* of icebergs covered the North Atlantic Ocean, causing the so-called Heinrich events, which induced a rapid weakening of the Atlantic Meridional Overturning Circulation (AMOC) (Heinrich, 1988; Broecker, 1994; Ganopolski and Rahmstorf, 2002; Hemming, 2004).

Although most of the records documenting this rapid climate variability are concentrated in the North Atlantic region, a number of studies from the tropical Atlantic and Pacific Oceans point towards a linkage between cooling episodes in the North Atlantic records and millennial-scale changes in Sea Surface Temperature (SST), humidity and marine productivity in the tropics (Baker et al., 2001; Haug et al., 2001; Wang et al., 2004, 2007; Muller, 2006; Clement and Peterson, 2008). This evidence suggests a connection between high and low latitudes to rapid climatic oscillations during last glacial cycle, which likely involved a tied ocean–atmosphere coupling (Oppo et al., 2003). Some tropical and subtropical records of MIS 3 from Africa, South America and Australia show changes in precipitation patterns during Heinrich Stadials (HS) (Wang et al., 2004; Muller, 2006; Tierney et al., 2008). MIS 3 changes in SST and salinity in the West Equatorial Pacific have been interpreted as changes in the super El Niño–Southern Oscillation (ENSO) state (Stott et al., 2002), whereas others have regarded changes in tropical rainfall as evidence of latitudinal displacements of the Intertropical Convergence Zone (ITCZ) (Wang et al., 2007; Leduc et al., 2009).

Currently, there are few records available with an appropriate temporal resolution to characterize millennial-scale changes in tropical and subtropical areas (Arz et al., 1998; Peterson et al., 2000; Rosenthal et al., 2000; Haug et al., 2001; Wang et al., 2004, 2007; Cruz et al., 2005; Muller et al., 2006; Conroy et al., 2008). However, none of these records is adequate for tracking changes over Central Pacific, an area were pa-

CPD
11, 1407–1435, 2015

leoceanographical records are absent due to the extremely low marine primary productivity which makes the sediments unsuitable for such climatic reconstructions. Easter Island is situated in a key area for understanding South Pacific climate, filling a regional gap without proper paleoclimatic registers suitable to understand MIS 3 climate. The Rano Aroi peatland is located in the highest area of Easter Island and its environmental history and has been extensively studied from an interdisciplinary approach (Margalef et al., 2013, 2014). The hydroclimatic sensitivity of this mire, the broad multiproxy dataset available and the adequate resolution of its record makes Rano Aroi an excellent location to provide a comprehensive reconstruction of the South Pacific Convergence Zone (SPCZ) evolution during the MIS 3.

In order to better understand the regional ocean-atmosphere connections, the Rano Aroi record dataset (Margalef et al., 2013, 2014) is compared to a new suite of equatorial SST gradient estimations based on previously published SST reconstructions. We also compare the Rano Aroi record to high latitude datasets from the Northern and Southern Hemispheres to discuss the inter-latitudinal connections responsible for the propagation of rapid climate variability during MIS 3.

2 Study site

Easter Island (Chile, 27°07′ S, 109°22′ W), or Rapa Nui in the local indigenous language, is a small Miocene volcanic island in the South Pacific Ocean, 3510 km from the South American continent (Fig. 1). The climate at the study site is subtropical, with average monthly temperatures oscillating between 18 and 24 °C and with a highly variable annual rainfall (mean value 1130 mm) (Junk and Claussen, 2011).

The climate on Easter Island displays low seasonality. However, a seasonal latitudinal migration of the ITCZ, SPCZ and westerly storm track is responsible for higher precipitation rates between March and June. Two processes are responsible for rainfall formation over Easter Island: (1) cyclonic storms associated with SPCZ dynamics and pushed eastwards by the Southern Westerlies (Sáez et al., 2009, Junk and Claussen,

CPD
11, 1407–1435, 2015

2011), and (2) land-sea breeze convection storms (Junk and Claussen, 2011). An analysis of the 1987–2005 satellite data performed within the framework of the HOAPS-3 project indicates that Easter Island lies at the active edge of the SPCZ, with associated precipitation rates between 657 and 803 mm yr^{-1} (Andersson et al., 2007; Junk and Claussen, 2011). This analysis of the HOAPS-3 dataset excluded topographic effects, and for this reason, the disparity between estimated and recorded rainfall rates has been attributed to the contribution of island topography to convective storms (Junk and Claussen, 2011).

Paleoenvironmental studies from Easter Island have traditionally been based on pollen analyses (Flenley and King, 1984; Flenley et al., 1991; Dumont et al., 1998; Butler et al., 2004; Gossen, 2007; Azizi and Flenley, 2008; Horrocks and Wozniak, 2008; Mann et al., 2008; Cañellas-Boltà et al., 2013) and macrofossils remains (Dumont et al., 1998; Orliac and Orliac, 1998, 2000; Peteet et al., 2003; Mann et al., 2008; Cañellas-Boltà et al., 2012), which have allowed the reconstruction of regional paleoclimatic and paleoenvironmental conditions from the last glacial period to the Holocene (Flenley et al., 1991; Azizi and Flenley, 2008; Rull et al., 2010a). Recent multiproxy studies which combined sedimentological, mineralogical, geochemical and biological data, have also documented hydrological changes in Easter Island since ca. 34 kyr cal BP (Sáez et al., 2009; Cañellas-Boltà et al., 2012, 2013) and since MIS 4 (Margalef et al., 2013).

The Rano Aroi mire (27°5′36″ S–109°22′25″ W, 430 m elevation) is located in a volcano crater near the highest summit of the island, Mauna Terevaka (511 m a.s.l.) (Fig. 1). The chemical composition of the flowing Rano Aroi outlet (lightly acidic, pH = 5.5–6.5) is similar to that of the region's groundwater. Water isotopic data (δ^{18}O and δ^{2}H) indicates that waters are renewed through discharge from an aquitard, which is quite sensitive to seasonal variations in precipitation (Herrera and Custodio, 2008). The hydrology configuration in this region indicates that Rano Aroi is a self-sealing mire fed by deeper discharging groundwater rather than by interflow (Margalef et al., 2013).

CPD
11, 1407–1435, 2015

3 Methodology

Detailed information about field campaign, peat sampling and chemical analyses (TC, TN, $\delta^{13}C$, Fe, Ti and Ca) can be found in Margalef et al. (2013). $\delta^{13}C$ variability ($\delta^{13}C_{res}$) was analyzed by subtracting a 19-sample mean running average from the raw $\delta^{13}C$ data to highlight high-frequency events compared to long-term tendencies. This 6-variables dataset was selected because it permits to reconstruct the main environmental processes controlling Rano Aroi geochemical evolution (Margalef et al., 2013).

A new age model for the bottommost part of the record has been set up using the ages provided at Margalef et al. (2013). Chronologic uncertainties are one of the most common troubles on studies comprising the MIS 3 period, because they are situated beyond the radiocarbon limit. In this study we estimate age-depth relationship using a mixed-effect model and constant variance (Heegaard et al., 2005) using R software (R Development Core Team, 2011). This method, highlights not only the error estimate of the sample, but also the uncertainty related to how representative the obtained age is in relation to the object level. The procedure combines two random effects (within-object variance and between-object variance) obtaining better confidence intervals than other methodologies for modeling ages beyond the dating limit (Heegaard et al., 2005). This mixed regression method has been run to model the age-depth relation in the well constrained part of the record (235–750 cm depth). The obtained model, was used to determine the age of the bottommost part of the register, older than the radiocarbon dating limit.

Statistical treatment of the data was performed with R software (R Development Core Team, 2011) and the "vegan" package (Oksanen et al., 2005). Principal component analysis (PCA) on the data that represented the MIS 3 was run to extract the main components of variability of the geochemical data (TC, TN, $\delta^{13}C_{res}$, Fe, Ti and Ca), standardizing and omitting samples with missing values. As in Margalef et al. (2013) and because of the different sampling resolution of the XRF dataset (2 mm) and of the

CPD
11, 1407–1435, 2015

geochemical data (5 cm), the XRF dataset was resampled at 5 cm intervals to make both datasets comparable. The resampling involved obtaining the mean values of the Ca, Ti and Fe measurements in every 5 cm.

A new gradient estimation between the Western and Eastern Equatorial Pacific have been calculated using previously published SST datasets from sites ODP 1240 site in the Eastern Equatorial Pacific Ocean (Pena et al., 2008) and core MD97-2141 in the Western Pacific Ocean (Dannenmann et al., 2003). The temperature calibrations were those used by authors in their original publications and have been interpreted to reflect mostly annual average temperature (Dannenmann et al., 2003; Pena et al., 2008). Previously to the calculation, all the SST records were resampled at common age interval (every 250 years) using R software (R Development Core Team, 2011). For an extended explanation of the criteria followed to choose these sites to the gradient see the Supplement.

4 Results

4.1 Geochemistry and peat facies

According to Margalef et al. (2013, 2014), the Rano Aroi sequence ARO 06 01 is composed of radicel peat sensu Succow and Joosten (2001), made of fine roots (diameter < 1 mm), with < 10 % of larger remains, (*Cyperaceae*, *Poaceae* and *Polygonaceae*). General description based on geochemistry, peat type, plant components and color has been used to define four facies (Margalef et al., 2013). The facies A (reddish peat) is characterized by low TN, Fe and Ti values, elevate carbon to nitrogen (C / N) ratio and a $\delta^{13}C$ signature close to C_3 plants values (Fig. 2). On the other hand, facies B (granulated muddy peat) is described as coarse and brown peat, mainly made of roots and rootlets and characterized by low terrigenous content. High C/N ratios, low Fe and Ti content and $\delta^{13}C$ values ranging from −14 to −26 ‰ differentiate this facies (Fig. 2). Facies C (organic mud) is characterized by thin layers interbedding Facies B and dis-

CPD
11, 1407–1435, 2015

playing high Fe and Ti values, high TN and relatively light $\delta^{13}C$ values (−14 to −22 ‰). Facies D (sapric peat) appears as dark and fine grains and contains organic matter with advanced degradation signs. This facies is primarily defined by high Fe and Ca content (Fig. 2).

SEM analysis of Facies C sand grains revealed the presence of plagioclase and quartz grains in the coarse fraction (> 500 µm). Silt particles (< 50 µm) were present on Facies B and C, mainly compound of ilmenite, rutile and silica. SEM analysis of the terrigenous content of the Facies D showed that the mineral fraction below 30 µm consisted of a mixture of Al, Fe, Mn oxides and organic bounded Ca as well as other organic compounds.

4.2 Age model

A detailed description of main features of Rano Aroi age model can be found in Margalef et al. (2013). The application of mixed-effect model (Heegaard et al., 2005), instead a an extrapolation, introduces slight changes, preserving general patterns but improving the age determination and associated errors of the record bottom part, that lies beyond the radiocarbon limit (Fig. 3).

We have restricted our study of millennial-scale variability (including stadial-interstadial oscillations) to the time window between an stratigraphic discontinuity at 38 kyr cal BP (see Margalef et al., 2013, 2014) and 65 kyr BP, so the MIS3/MIS4 transition (59.4 kyr BP, Svensson et al., 2008) is also included in our study (Fig. 2). The facies and stratigraphy present in the well constrained part of the record selected – between 38.5 and 55 kyr (4.31–8.75 m) – and the portion that is older than radiocarbon limit are homogenous. Moreover, there were no evidence of drought episodes by any geochemical, microscopic or macroscopic observations in the lower part of the record, what supports age extrapolation by the mixed-effect model approach (Heegaard et al., 2005).

CPD
11, 1407–1435, 2015

4.3 Principal component analysis result

Principal Component Analysis (PCA) was performed on a dataset composed of 6 variables (TN, TC, $\delta^{13}C_{res}$, Ti, Fe and Ca) and 142 samples, which represented the aforementioned 38.5 to 65 kyr BP period (Figs. 2 and 4). The first component explained 34.7 % and the second component explained an additional 30.6 % of the total variance (Fig. 4). Ti, Fe and Ca contributed positively to the first component, whereas TN and $\delta^{13}C_{res}$ values are found at the opposite end of the first component. TN and Ti are found at the positive end of PC2 (Figs. 2 and 4), whereas Ca and $\delta^{13}C_{res}$ contributed negatively to the second component. Facies C scores are related to Ti, TN and $\delta^{13}C_{res}$ variability, indicating that they are well represented by PC2 (Figs. 2 and 4).

4.4 SST gradient across the equatorial Pacific

The current SST gradient between the E–W locations of the equatorial Pacific Ocean oscillates from 1.2 °C in boreal winter to 6 °C in boreal summer when the eastern equatorial upwelling system is fully developed, while the annual average SST gradient is 3.3 °C (World Ocean Data 2009; Locarnini et al., 2010). The calculated SST gradient between the western and eastern sites shows average values of 4.4 °C, with maximum values reaching 6 °C and minimum values at approximately 3 °C (Fig. 5). According to their SST-calibrations the error of these SST gradients is considered to be better than ±0.6 °C while the discussion of this SST gradient mostly focuses on those changes which are above 1 °C or even larger (> 2 °C).

CPD
11, 1407–1435, 2015

5 Discussion

5.1 Rano Aroi paleoenvironmental reconstruction

As stated in Margalef et al. (2013) and Margalef et al. (2014) three main environmental and hydrologic phases can be distinguished on the basis of the characterization of the four facies:

Open water phase represented by Facies C. During this phase, coarse (> 500 m) sandy particles from volcanic soils were transported through dense mire vegetation and deposited at the center of this sedimentary deposit. The presence of these sandy particles would involve high precipitation rates. Low $\delta^{13}C_{res}$ isotopic values also reinforce the hypothesis that Facies C are tracking enhanced precipitation events (Margalef et al., 2014). This open water phase is tracked by high PC2 values (Figs. 2 and 4) what allows us to use this component as rainfall indicator.

Long-term stable and near-surface water table phase evidenced by Facies A and B. This phase led the constant accumulation of peat sediments which were deposited in a *kettle hole* mire (Margalef et al., 2014), under accumulation conditions similar to the present Rano Aroi. Peat presented a low degree of humidification owing to lower rainfall conditions with respect to the previous ones. This stable and sub-surficial water table conditions are reflected in the PC2 component by intermediate values.

A third environmental phase is represented by Facies D and can be interpreted as a result of diagenesis of previously accumulated peat (Fig. 2, Margalef et al., 2013). Iron and calcium were incorporated into the mire as terrigenous particles, but affected by post-depositional remobilization with water movement and redox changes. Both chemical elements were incorporated into organic matter by complexation as Fe–Ca-humates under oxic conditions (Shotyk et al., 1996; Margalef et al., 2014).

CPD
11, 1407–1435, 2015

5.2 Precipitation patterns over the tropical and subtropical Pacific during MIS 3

As previously stated in Margalef et al. (2014), the present second component of variability (PC2) adequately summarizes the occurrence of a waterlogged environment and higher precipitation periods and, therefore, it can be used as a non-quantitative humidity-index. Following this premise, the occurrence of 6 wet events – labeled Ar1 to Ar6 – have been identified between 38.5 and 65 kyr BP based on their high PC2 values (Fig. 2). Three of these wet periods (Ar2, Ar4 and Ar6) are particularly outstanding. These periods are characterized by an abrupt onset and last for approximately 2000 years. The other three wet events (Ar1, Ar3 and Ar5) are also characterized by an abrupt start but are of minor intensity and duration, lasting approximately 1000 years or less (Figs. 5–6). A comparison of the PC2 scores of the Rano Aroi record with other well-established climate records from the Northern and Southern Hemispheres indicates that the three major Rano Aroi events can tentatively be correlated with the North Atlantic HS 5 (ca. 47 kyr BP), 5a (ca. 53 kyr BP) and 6 (ca. 60 kyr BP), whereas the three minor events can be correlated with other DO stadials (Figs. 5–6). Wet events Ar1, Ar2 and Ar3, that are located within the well-constrained part of the age model, show a good correlation with cold phases at North Atlantic coinciding with DO stadials and Heinrich events. This pattern is maintained in the bottommost part of the record, therefore supporting the Rano Aroi chronological framework (Figs. 5–6).

A strong argument that reinforces the link between the Rano Aroi wet events and the DO stadials is that is mechanistically coherent with the regional atmospheric and oceanographic reconstructions from independent proxy records. Some of the most solid evidence of atmospheric teleconnections for the DO oscillations come from Northern Hemisphere records such as speleothem records from the Hulu cave speleothems in China (32°30′ N; Wang et al., 2001), the reflectance record from the Cariaco basin, northern Venezuela (10°43′ N, Peterson et al., 2000; Haug et al., 2001) and changes in surface salinity in the Sulu sea indicated by core MD 97-2141 (8°48′ N, Oppo et al., 2003; Dannenmann et al., 2003; Rosenthal et al., 2000). All of these records consis-

CPD
11, 1407–1435, 2015

tently indicate the dominance of dry conditions during the HS and other DO stadials (Fig. 6). These events have been associated with the opposite behavior in the Southern Hemisphere, as documented by wet events recorded in Northern Brazil travertine formations (Wang et al., 2007) and in marine cores offshore of the South American Atlantic coast (3°40′ S, Arz et al., 1998), which correlate with the Rano Aroi major wet events (Fig. 6). A similar climatic pattern has been described by Muller et al. (2008b) in the Lynch crater (17° S) peat record in North Australia over the last 45 kyr cal BP. This tropical asynchrony between the two hemispheres has been explained by latitudinal migrations of ITCZ (Peterson et al., 2000; Tierney et al., 2008; Leduc et al., 2009). Changes in the AMOC and atmospheric coupling during DO stadials (interstadials) seems to provoke the southward (northward) displacement of ITCZ (Zhang and Delworth, 2005; Clement and Peterson, 2008; Chiang and Bitz, 2005; Timmermann et al., 2005). Other authors propose that main changes in ITCZ migration and in SST temperatures of tropical Pacific were also linked to monsoon fluctuations. For example, Oppo and Sun (2005) suggested the connection between periods of reduced precipitation due to a weaker monsoon over South China Sea during HS.

Although several studies support the occurrence of these ITCZ migrations, changes in the position of the SPCZ low-pressure belt are less well known. In spite of both structures are intimately related, precipitation over Easter Island is primarily determined by the arrival of cyclogenic storms generated on the SPCZ (Junk and Claussen, 2011). Easter Island hydrologic changes might record then, millennial-scale oscillations in the expansion of the SPCZ, coupled with ITCZ migrations. This could be explained by an eastward expansion of the SPCZ associated to the southwards shift in the ITCZ during MIS 3, in a Pacific configuration resembling the austral summer. However, stronger efforts on finding records capable to track SPCZ activity during MIS 3 and modeling support are required to completely understand MIS 3 Central Pacific configuration. Rano Aroi record suggests that abrupt hydrological oscillations were present not only during HS but also during other shorter DO stadials (Fig. 6). Rano Aroi record also shows how hydrological conditions underwent abrupt changes meaning a rapid response to

CPD
11, 1407–1435, 2015

AMOC. These abrupt shifts differed from the Southern Hemisphere thermal response, which involved gradual onsets and terminations, as seen in Antarctic ice core records (Schmittner et al., 2003; Blunier et al., 1998; Blunier and Brooks, 2001; EPICA, 2006) (Fig. 6).

5.3 Changes in the E–W equatorial SST gradient of the Pacific Ocean during MIS 3

Some climate models propose that North Atlantic cold events eventually lead to changes in the Walker circulation (Zhang and Delworth, 2005). Following Zhang and Delworth (2005) modeling, the southeastern trade winds were weakened during North Atlantic melting events, and, consequently, the upwelling in the eastern equatorial Pacific was drastically reduced what could be related to ITCZ migration and to ENSO-state changes. This hypothesis can be tested by examining a reconstruction of the SST gradient across the equatorial Pacific using the temperature differences between the eastern cold tongue and the western warm pool. Low values in the SST gradient would be consistent with a weakening of the Walker circulation and should reflect periods of diminished upwelling activity in the eastern equatorial Pacific. Eastern Pacific upwelling is responsible for the upward transport of relatively cold and salty waters, whereas the very warm and fresh waters are dominant in the western Pacific warm pool (Kessler, 2006). By contrast, higher SST gradient values should be consistent with intensified upwelling in the eastern equatorial Pacific, whereas a reduced gradient indicates more homogenous hydrographic conditions along the Equator.

The obtained gradient present lower values of zonal SST gradient coincident with the Rano Aroi wet events (Fig. 5). Consequently, the lower equatorial SST gradient associated to DO stadials is consistent with a muted upwelling in the eastern Equatorial Pacific and a weaker Walker circulation, which ultimately would favors a southward shift in the ITCZ and an eastward expansion of the SPCZ, as is interpreted from the Rano Aroi record. This configuration would be in line with the already proposed ENSO-like state during cold North Atlantic periods and the southward migration of the ITCZ based

CPD
11, 1407–1435, 2015

in climate models (Clement and Cane, 1999) and also in proxy reconstructions (Haug et al., 2000; Fedorov and Philander, 2000; Koutavas et al., 2006; Zuraida et al., 2009; Bolliet et al., 2011). An analogous correlation can be described based on present day instrumental data: extreme El Niño events are characterized by a mean southward migration of the Pacific ITCZ (Haug et al., 2000; Fedorov and Philander, 2000) and by an eastward and northward migration of the SPCZ (Vincent et al., 2009).

Nevertheless, other models consider these atmospheric mechanisms less relevant and instead highlight the role of the ocean's circulation through a global baroclinic adjustment when the North Atlantic cools and when there is a reduction in the AMOC. These models suggest that North Atlantic water density variations can lead to changes in the global thermocline within a few years to decades (Huang et al., 2000). These authors describe changes in the Pacific thermocline and argue that, despite the occurrence of climatic fluctuations that can be explained without invoking a link between El Niño and stadials, the existence of such a linkage cannot be excluded (Huang et al., 2000; Timmermann et al., 2005).

5.4 Tropical connections to Southern Hemisphere high latitudes

The southward migration of the ITCZ results in both a reinforcement of the equator-to-pole pressure gradient over the Southern Hemisphere and in an intensification of the Southern Westerlies (SW) (Toggweiler et al., 2006; Anderson and Carr, 2010; Heirman, 2011). Changes in the position and intensity of the SW during MIS 3 should have promoted storminess over Central Pacific and contributed to an eastward movement of storms generated under the SPCZ. Another process intimately linked with the SW is the formation of intermediate water masses in the Southern Ocean. Changes in the formation rate of Antarctic Intermediate Water (AAIW) associated with DO cycles have been described in a marine record from Chatman Rise, East New Zealand (MD97–2120, 45°32.06′ S, 174°55.85′ E, Pahnke and Zahn, 2005) on the basis of the benthic foraminiferal δ^{13}Crecord (Figs. 1 and 6). It has been demonstrated that periods of increased AAIW production were in phase with Southern Hemisphere warming

CPD
11, 1407–1435, 2015

and southward shifts of the ITCZ (Pahnke and Zahn). During DO stadials, the Antarctic continent and Southern Ocean warmed as a result of the bipolar seesaw, and, consequently, Antarctic sea ice retreated (Anderson and Carr, 2010; Skinner et al., 2010). This reduced sea ice extent would contribute to enhanced upwelling of circumpolar deep water and to a more efficient downwelling of AAIW (Toggweiler et al., 2006; Anderson and Carr, 2010; Skinner et al., 2010) (Fig. 1). A recent study using Nd isotopes as a proxy for water mass provenance demonstrated that an increased export of AAIW from the Southern Ocean to tropical regions occurred during Northern Hemisphere cold periods such as HS (Pena et al., 2013). This oceanic circulation scenario also induced the release of oceanic CO_2, which was stored in poorly ventilated deep-water masses, to the atmosphere (Anderson and Carr, 2010; Skinner et al., 2010). In the context of the Rano Aroi wet events, these specific oceanic conditions in the Southern Ocean during DO stadials could have cause increased precipitation over Central Pacific.

6 Conclusions

The Rano Aroi peat record provides a unique opportunity to understand the evolution of South Pacific climate during the late Pleistocene. This record contains information concerning climate variability during MIS 3 and is located thousands of kilometers away from other continental and marine paleoclimatic records. Six main humid events occurred in Rano Aroi during MIS 3 as a result of an eastward expansion of the SPCZ and they have been associated to the North Atlantic HS but also to other minor DO stadials.

Anti-phase changes in precipitation and hydrology have been observed in low-latitude areas of the Northern and Southern Hemispheres. These changes have already been linked to North Atlantic cold stadials through a southward displacement of the ITCZ, as described by several studies based on both numerical climate models and environmental reconstructions from Circum-Pacific sites. The Rano Aroi record

CPD
11, 1407–1435, 2015

allowed us to propose that these stadials were also associated with an eastward expansion of the SPCZ, highlighting a close coupling between the migration of the ITCZ and potentially the SPCZ on millennial timescales. The abrupt character of the Rano Aroi humid events demonstrates the rapid atmospheric response of the tropical regions to the DO-related sudden changes in the AMOC, in contrast to the more progressive heat redistribution in the Southern Ocean led by the bipolar seesaw. The Rano Aroi wet events have been correlated with periods of a reduced SST gradient along the Equator, suggesting that more humid conditions over the Easter Island region occurred when the Walker circulation was reduced. These atmosphere-ocean connections in the tropical Pacific could be considered analogous to modern El Niño conditions. Associated changes in the Southern Ocean with strengthened Southern Westerlies, enhanced AAIW production and sea ice retreat during DO stadials, could have also reinforced the SPCZ extension over Easter Island.

The Supplement related to this article is available online at doi:10.5194/cpd-11-1407-2015-supplement.

Acknowledgements. This research was funded by the Spanish Ministry of Science and Education through the projects LAVOLTER (CGL2004–00683/BTE), GEOBILA (CGL2007–60932/BTE), PALEONAO (CGL2010–15767) and RAPIDNAO (CGL2013–40608R) and through undergraduate CSIC JAEPre grant (BOE 04 March 2008) to Olga Margalef. We would like to thank Hans Joosten, Alex Barthemles, John Couwenberg, Martin Theuerkauf, Susanne Abel, Almut Spangenberg, Dirk Michaelis and René Dommain for their help and contributions to the peatland characterisation during O.M.'s stay at the University of Greifswald.

CPD
11, 1407–1435, 2015

References

Andersson, A., Bakan, S., Fennig, K., Grassl, H., Klepp, C. P., and Schulz, J.: Hamburg Ocean Atmosphere Parameters and Fluxes from Satellite Data – HOAPS-3 – monthly mean, World Data Center for Climate 3097, 385–393, doi:10.1594/WDCC/HOAPS3_MONTHLY, 2007.

Anderson, R. F. and Carr, M. E.: Uncorking the Southern Ocean's Vintage CO_2, Science, 328, 1117–1118, 2010.

Arz, H. W., Pätzold, J., and Wefer, G.: Correlated millennial-scale changes in surface hydrography and terrigenous sediment yield inferred from last-glacial marine deposits off Northeastern Brazil, Quaternary Res., 50, 157–166, 1998.

Azizi, G. and Flenley, J. R.: The last glacial maximum climatic conditions on Easter Island, Quatern. Int., 184, 166–176, 2008.

Baker, P. A., Rigsby, C. A., Seltzer, G. O., Fritz, S. C., Lowenstein, T. K., Bacher, N. P., and Veliz, C.: Tropical climate changes at millennial and orbital time scales on the Bolivian Altiplano, Nature, 409, 698–701, 2001.

Blunier, T. and Brook, E. J.: Timing of millennial-scale climate change in Antarctica and Greenland during the last glacial period, Science, 291, 109–112, 2001.

Blunier, T., Chappellaz, J., Schwander, J., Dällenbach, A., Stauffer, B., Stocker, T. F., Raynaud, D., Jouzel, J., Clausen, H. B., Hammer, C. U., and Johnsen, S. J.: Asynchrony of Antarctic and Greenland climate change during the last glacial period, Nature, 394, 739, 1998.

Bolliet, T., Holbourn, A., Kuhnt, W., Laj, C., Kissel, C., Beaufort, L., Kienast, M., Andersen, N., and Garbe-Schönberg, D.: Mindanao Dome variability over the last 160 kyr: episodic glacial cooling of the West Pacific Warm Pool, Paleoceanography, 26, PA1208, doi:10.1029/2010PA001966, 2011.

Broecker, W.: Massive iceberg discharges as triggers for global climate change, Nature, 372, 421–424, 1994.

Butler, K., Prior, C. A., and Flenley, J. R.: Anomalous radiocarbon dates from Easter Island, Radiocarbon, 46, 395–405, 2004.

Cañellas-Boltà, N., Rull, V., Sáez, A., Margalef, O., Giralt, S., Pueyo, J. J., Birks, H. H., Birks, H. J. B., and Pla-Rabes, S.: Macrofossils in Raraku Lake (Easter Island) integrated with sedimentary and geochemical records: towards a paleoecological synthesis, Quaternary Sci. Rev., 34, 113–126, 2013a.

CPD
11, 1407–1435, 2015

Cañellas-Boltà, N., Rull, V., Sáez, A., Margalef, O., Bao, R., Pla-Rabes, S., Blaauw, M., Valero-Garcés, B., and Giralt, S.: Vegetation changes and human settlement of Easter Island during the last millennia: a multiproxy study of the Lake Raraku sediments, Quaternary Sci. Rev., 72, 36–48, 2013b.

Chiang, J. C. H. and Bitz, C. M.: Influence of high latitude ice cover on the marine Intertropical Convergence Zone, Clim. Dynam., 25, 477–496, doi:10.1007/s00382-005-0040-5, 2005.

Clement, A. C. and Peterson, L. C.: Mechanisms of abrupt climate change of the last glacial period, Rev. Geophys., 46, RG4002, doi:10.1029/2006RG000204, 2008.

Conroy, J. L., Overpeck, J. T., Cole, J. E., Shanahan, T. M., and Steinitz-Kannan, M.: Holocene changes in eastern tropical Pacific climate inferred from a Galápagos lake sediment record, Quaternary Sci. Rev., 27, 1166–1180, 2008.

Cruz Jr, F. W., Burns, S. J., Kamman, I., Sharp, W. D., Vuille, M., Cardoso, A. O., Ferrari, J. A., Silva Dias, P. L., and Viana Jr., O.: Insolation-driven changes in atmopsheric circulation over the past 116000 years in subtropical Brazil, Nature, 434, 63–66, 2005.

Dannenmann, S., Linsley, B. K., Oppo, D. W., Rosenthal, Y., and Beaufort, L.: East Asian monsoon forcing of suborbital variability in the Sulu Sea during marine isotope stage 3: Link to Northern Hemisphere Climate, Geochem. Geophy. Geosy., 4, 1–13, 2003.

Dansgaard, W., Johnsen, S. J., Clausen, H. B., Dahl-Jensen, D., Gundestrup, N. S., Hammer, C. U., Hvidberg, C. S., Steffensen, J. P., Sveinbjörnsdottir, A. E., Jouzel, J., and Bond, G.: Evidence for general instability of past climate from a 250 kyr ice core record, Nature, 364, 218–220, 1993.

Dong, B.-W. and Sutton, R. T.: Adjustment of the coupled ocean-atmosphere system to a sudden change in the thermohaline circulation, Geophys. Res. Lett., 29, 2002.

Dumont, H. J., Cocquyt, C., Fontugne, M., Arnold, M., Reyss, J.-L., Bloemendal, J., Oldfield, F., Steenbergen, C. L. M., Korthals, H. J., and Zeeb, B. A.: The end of moai quarrying and its effect on Rano Raraku, Easter Island, J. Paleolimnol., 20, 409–422, 1998.

EPICA Community Members: One-to-one coupling of glacial climate variability in Greenland and Antarctica, Nature, 444, 195–198, 2006.

Fedorov, A. V. and Philander, S. G.: Is El Niño changing?, Science, 288, 1997–2002, 2000.

Flenley, J. R. and King, S. M.: Late Quaternary pollen records from Easter Island, Nature, 307, 47–50, 1984.

CPD
11, 1407–1435, 2015

Flenley, J. R., King, S. M., Jackson, J., Chew, C., Teller, J. T., and Prentice, M. E.: The late quaternary vegetational and climatic history of Easter Island, J. Quaternary Sci., 6, 85–115, 1991.
Ganopolski, A. and Rahmstorf, S.: Abrupt glacial climate changes due to stochastic resonance, Phys. Rev. Lett., 88, 3, 2002.
Gossen, C.: Report: the mistery lies in the Scirpus, Rapa Nui Journal, 21, 105–110, 2007.
Haug, G. H., Hughen, K. A., Sigman, D. M., Peterson, L. C., and Röhl, U.: Southward Migration of the intertropical convergence zone through the Holocene, Science, 293, 1304–1308, 2005.
Heegaard, E., Birks, H. J. B., and Telford, R. J.: Relationships between calibrated ages and depth in stratigraphical sequences: an estimation procedure by mixed-effect regression, Holocene, 15, 612–618, 2005.
Heinrich, H.: Origin and consequence of cyclic ice rafting in the northeast Atlantic Ocean during the past, 130,000 years, Quaternary Res., 29, 142–152, 1988.
Heirman, K.: "A wind of Change", Changes in position and intesity of the Southern Hemisphere Westerlies during oxygen isotope stages 3, 2 and 1, Ph.D. Thesis, University of Gent, Ghent (Belgium), 2011.
Hemming, S. R.: Heinrich events: massive late pleistocene detritus layers of the North Atlantic and their global climate imprint, Rev. Geophys., 42, RG1005, 2004.
Herrera, C. and Custodio, E.: Conceptual hydrogeological model of volcanic Easter Island (Chile) after chemical and isotopic surveys, Hydrogeol. J., 16, 1329–1348, 2008.
Horrocks, M. and Wozniak, J. A.: Plant microfossil analysis reveals disturbed forest and mixed-crop, dryland production system at Te Niu, Easter Island, J. Archaeol. Sci., 35, 126–142, 2008.
Huang, R. X., Cane, M. A., Naik, N., and Goodman, P.: Global adjustment of the thermocline in response to deepwater formation, Geophys. Res. Lett., 27, 759–762, 2000.
Joosten, H. and Clarke, D.: Wise Use of Mires and Peatlands – Background Principles including a Framework for Decision-Making, International Mire Conservation Group and International Peat Society, Saarijärvi, Finland, 2002.
Junk, C. and Claussen, M.: Simulated climate variability in the region of Rapa Nui during the last millennium, Clim. Past, 7, 579–586, doi:10.5194/cp-7-579-2011, 2011.
Kessler, W. S.: The circulation of the eastern tropical Pacific: a review, Prog. Oceanogr., 69, 181–217, 2006.

CPD
11, 1407–1435, 2015

Koutavas, A., Menocal, P. B., and Lynch-Stieglitz, J.: Holocene trends in tropical Pacific sea surface temperatures and the El Niño–Southern Oscillation, 13, 22–23, 2006.
Lea, D. W., Pak, D. K., Belanger, C. L., Spero, H. J., Hall, M. A., and Shackleton, N. J.: Paleoclimate history of Galápagos surface waters over the last 135,000 yr, Quaternary Sci. Rev., 25, 1152–1167, 2006.
Leduc, G., Vidal, L., Tachikawa, K., and Bard, E.: ITCZ rather than ENSO signature for abrupt climate changes across the tropical Pacific?, Quaternary Res., 72, 123–131, 2009.
LeGrande, A. N. and Schmidt, G. A.: Global gridded data set of the oxygen isotopic composition in seawater, Geophys. Res. Lett., 33, L12604, 2006.
Locarnini, R., Mishonov, A., Antonov, J., Boyer, T., Garcia, H., Baranova, O., Zweng, M., and Johnson, D.: World Ocean Atlas, edited by: NOAA Atlas NESDIS 68, U. S. Government Printing Office, Washington, D.C, 2010.
Mann, D., Edwards, J., Chase, J., Beck, W., Reanier, R., Mass, M., Finney, B., and Loret, J.: Drought, vegetation change, and human history on Rapa Nui (Isla de Pascua, Easter Island), Quaternary Res., 69, 201–206, 2008.
Margalef, O. Cañellas-Boltà, N., Pla-Rabes, S., Giralt, S., Pueyo, J. J., Joosten, H., Rull, V., Buchaca, T., Hernández, A., Valero-Garcés, B. L., Moreno, A., and Sáez, A.: A 70 000 year geochemical and paleoecological record of climatic and environmental change from Rano Aroi peatland (Easter Island), Global Planet. Change, 108, 72–84, 2013.
Margalef, O., Martínez-Cortizas, A., Pla-Rabes, S., Cañellas-Boltà, N., Pueyo, J. J., Alberto Sáez, A., Valero-Garcés, B., and Giralt, S.: Environmental processes in Rano Aroi (Easter Island) peat geochemistry forced by climate variability during the last 70 kyr, Palaeogeogr. Palaeocl., 414, 438–450, 2014.
Muller, J.: Reconstructing climate change of the last 55 kyr: the Lynch's Crater peat mire record, Ph.D. thesis, James Cook University, NE-QLD, Australia, 2006.
Muller, J., Wüst, R. A. J., Weiss, D. J., and Hu, Y.: Geochemical and stratigraphic evidence of environmental change at Lynch's Crater, Queensland, Australia, Global Planet. Change, 53, 269–277, 2006.
Muller, J., Kylander, M. E., Wüst, R. A., Weiss, D. J., Martinez Cortizas, A., LeGrande, N., Jennerjahn, T., Behling, H., Anderson, W. T., and Jacobson, G.: Possible evidence for wet Heinrich phases in tropical NE Australia: the Lynch's Crater desposit, Quaternary Sci. Rev., 27, 468–475, 2008.

CPD
11, 1407–1435, 2015

Oksanen, J., Kindt, R., Legendre, P., and O'Hara, R. B.: Vegan: Community Ecology Package, R package version 1.8–3, http://CRAN.R-project.org (last access 08 May 2013), 2006.
Oppo, D. W., and Sun, Y.: Amplitude and timing of sea-surface temperature change in the northern South China Sea: dynamic link to the East Asian monsoon, Geology, 33, 785–788, 2005.
Oppo, D. W., Linsley, B. K., Rosental, Y., Dannenmann, S., and Beaufort, L.: Orbital and suborbital climate variability in the Sulu Sea, western tropical Pacific, Geochem. Geophy. Geosy., 20, 1–20, 2003.
Orliac, C.: The woody vegetation of Easter Island between the early 14th and the mid-17th Centuries AD, in: Easter Island Archaeology: Research on Early Rapanui Culture, edited by: Stevenson, C. and Ayres, W., Easter Island Foundation, Los Osos, 2000.
Orliac, C. and Orliac, M.: The disappearance of Easter Island's forest: overexploitation or climatic catastrophe? in: Easter Island in Pacific Context: South Seas Symposium. Proceedings of the Fourth International Conference on Easter Island and East Polynesia, edited by: Stevenson, C., Lee, G., and Morin, F. J., Easter Island Foundation, Los Osos, 129–134, 1998.
Pahnke, K. and Zahn, R.: Southern Hemisphere water mass conversion linked with North Atlantic Climate Variability, Science, 307, 1741–1746, 2005.
Pena, L. D., Cacho, I., Ferretti, P., and Hall, M. A.: El Niño–Southern Oscillation–like variability during glacial terminations and interlatitudinal teleconnections, Paleoceanography, 23, PA3101, doi:10.1029/2008PA001620, 2008.
Pena, L. D., Goldstein, S. L., Hemming, S. R., Jones, K. M., Calvo, E., Pelejero, C., and Cacho, I.: Rapid changes in meridional advection of Southern Ocean intermediate waters to the tropical Pacific during the last 30 kyr, Earth Planet. Sc. Lett., 368, 20–32, 2013.
Peteet, D., Beck, W., Ortiz, J., O'Connell, S., Kurdyla, D., and Mann, D.: Rapid vegetational and sediment change from Rano Aroi crater, Easter Island, in: Scientific Exploration into the World's Environmental Problems in Microcosm, edited by: Loret, J. and Tanacredi, J. T., Kluwer Academic/Plenum Publ., New York, 81–92, 2003.
Peterson, L. C., Haug, G. H., Hughen, K. A., and Rohl, U.: Rapid changes in the hydrologic cycle of the tropical Atlantic during the last glacial, Science, 290, 1947–1951, 2000.
R Development Core Team: R: a language and environment for statistical computing. R Foundation for Statistical Computing, Vienna, Austria, available at: http://www.Rproject.org/ (last access: 08 May 2013), 2011.

CPD
11, 1407–1435, 2015

Rosenthal, Y., Oppo, D. W., Dannenmann, S., and Linsley, B. K.: Millennial-scale variability in western Pacific sea surface temperatures during glacial and Holocene climates, Eos Trans. AGU, Fall Meet. Suppl., 81, F656, 2000.
Rull, V., Cañellas-Boltà, N., Sáez, A., Giralt, S., Pla, S., and Margalef, O.: Paleoecology of Easter Island: Evidence and uncertainties, Earth-Sci. Rev., 99, 50–60, 2010a.
Rull, V., Stansell, N. D., Montoya, E., Bezada, M., and Abbott, M. B.: Palynological signal of the Younger Dryas in tropical Venezuelan Andes, Quaternary Sci. Rev., 29, 3045–3056, 2010b.
Sáez, A., Valero-Garcés, B., Giralt, S., Moreno, A., Bao, R., Pueyo, J. J., Hernández, A., and Casas, D.: Glacial to Holocene climate changes in the SE Pacific. The Raraku Lake sedimentary record (Easter Island, 27° S), Quaternary Sci. Rev., 28, 2743–2759, 2009.
Schmittner, A. Saenko, O. A., and Weaver, A. J.: Coupling of the hemispheres in observations and simulations of glacial climate change, Quaternary Sci. Rev., 22, 659–671, 2003.
Shotyk, W.: Peat bog archives of atmospheric metal deposition: geochemical evaluation of peat profiles, natural variations in metal concentrations, and metal enrichment factors, Environ. Rev., 4, 149–183, 1996.
Skinner, L. C., Fallon, S., Waelbroeck, C., Michel, E., and Barker, S.: Ventilation of the Deep Southern Ocean and deglacial CO_2 rise, Science, 328, 1147–1151, 2010.
Stott, L., Poulsen, C., Lund, S., and Thunell, R.: Super ENSO and global climate oscillations at millennial time scales, Science, 297, 222–226, 2002.
Svensson, A., Andersen, K. K., Bigler, M., Clausen, H. B., Dahl-Jensen, D., Davies, S. M., Johnsen, S. J., Muscheler, R., Parrenin, F., Rasmussen, S. O., Röthlisberger, R., Seierstad, I., Steffensen, J. P., and Vinther, B. M.: A 60,000 year Greenland stratigraphic ice core chronology, Clim. Past, 4, 47–57, doi:10.5194/cp-4-47-2008, 2008.
Succow, M. and Joosten, H.: Landschaftsökologische Moorkunde, Sweizerbart, Stuttgart, 622p., 2001.
Tierney, J. E., Russell, J. M., Huang, Y., Sinninghe Damsté, J. S., Hopmans, E. C., and Cohen, A. S.: Northern Hemisphere controls on tropical southeast African climate during the past 60 000 years, Science, 322, 252–255, 2008.
Timmermann, A., Krebs, U. Justino, F., Goosse, H., and Ivanochko, T.: Mechanisms for millennial-scale global synchronization during the last glacial period, Paleoceanography, 20, 4, 2005.
Toggweiler, J. R., Russell, J. L., and Carson, S. R.: Midlatitude westerlies, atmospheric CO_2, and climate change during the ice ages, Paleoceanography, 21, 1–15, 2006.

CPD
11, 1407–1435, 2015

Vincent, E., Lengaigne, M., Menkes, C. E., Jourdain, N. C., Marchesiello, P., and Madec, G.: Interannual vairiability of the South Pacific Convergence Zone and implications for tropical cyclone genesis, Clim. Dynam., 36, 1881–1896, 2009.

Wang, X., Auler, A. S., Edwards, R. L., Cheng, H., Cristalli, P. S., Smart, P. L., Richards, D. A., and Shen, C. C.: Wet periods in northeastern Brazil over the past 210 kyr linked to distant climate anomalies, Nature, 432, 740–743, 2004.

Wang, X., Auler, A. S., Edwards, R. L., Cheng, H., Ito, E., Wang, Y., Kong, X., and Solheid, M.: Millennial-scale precipitation changes in southern Brazil over the past 90,000 years, Geophys. Res. Lett., 34, 1–5, 2007.

Weiss, D., Shotyk, W., Rieley, J. O., Page, S. E., Gloor, M., Reese, S., and Cortizas-Martínez, A.: The geochemistry of major and selected trace elements in a forested peat bog, Kalimantan, SE Asia, and its implications for past atmospheric dust deposition, Geochim. Cosmochim. Ac., 66, 2307–2323, 2002.

Xie, S. P.: On the genesis of the equatorial annual cycle, J. Climate, 7, 2008–2013, 1994.

Yuan, X.: ENSO-related impacts on Antarctic sea ice: a synthesis of phenomenon and mechanisms, Antarct. Sci., 16, 415–425, doi:10.1017/S0954102004002238, 2004.

Zhang, R. and Delworth, L. T.: Simulated Tropical Response to a Substantial Weakening of the Atlantic Thermohaline Circulation, American Meterorological Society, 18, 1853–1860, 2005.

Zuraida, R., Holbourn, A., Nürnberg, D., Kuhnt, W., Dürkop, A., and Erichsen, A.: Evidence for Indonesian throughflow slowdown during Heinrich events 3–5, Paleoceanography, 24, doi:10.1029/2008PA001653, 2009.

CPD
11, 1407–1435, 2015

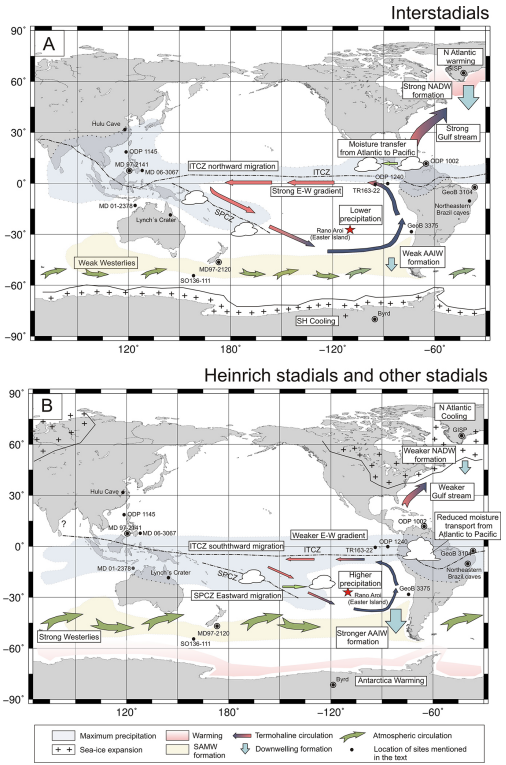

Figure 1. Oceanic and atmospheric spatial patterns of millennial-scale climate change events (see discussion, Sect. 5) that acted as climatic teleconnection mechanisms or feedbacks during MIS 3 interstadials (Map A) and HS (Map B). Black dots indicate the most relevant sites mentioned in the text, double circles indicate records also represented in Fig. 6 and Rano Aroi is designated as a red star.

CPD
11, 1407–1435, 2015

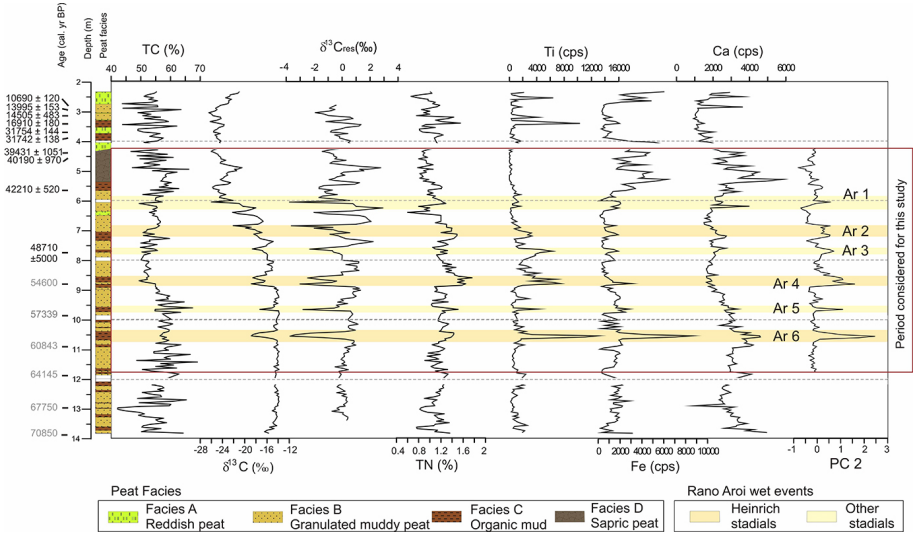

Figure 2. Geochemical proxies analyzed in ARO 06 01 core vs. depth. Peat facies and radiocarbon ages are indicated in the first column. Geochemical proxies: TC, TN, (in percentages), C/N ratio, and δ^{13}C (‰) is indicative of the origin of organic matter. Residual values of $\delta^{13}C_{res}$ (‰) are used to enhance the presence of δ^{13}C dips. Fe, Ti and Ca FRX measurements (in cps) and Fe/Ti, Ca/Ti ratios are also shown together with the scores of PC2.

CPD
11, 1407–1435, 2015

Millennial-scale precipitation variability over Easter Island during MIS 3

O. Margalef et al.

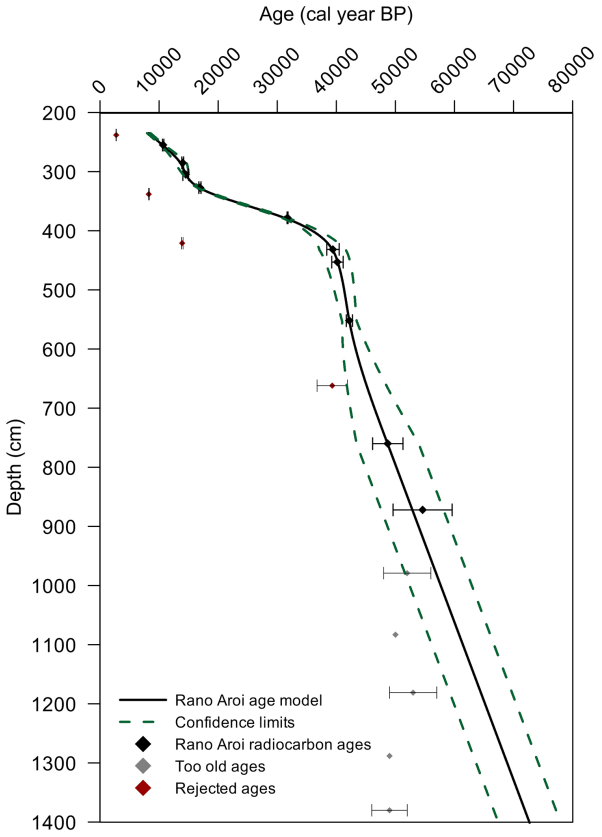

Figure 3. Rano Aroi age model. Samples from ARO 06 01. Ages in red were rejected by reflecting inversions (Margalef et al., 2013). Ages in grey lied beyond radiocarbon limit. Error bars for each point are shown. Black lines shows the result of the mixed-effect model performed between 235 and 750 cm depth and extrapolated until the bottommost part of the record. Green dashed line are showing the confidence limits.

CPD
11, 1407–1435, 2015

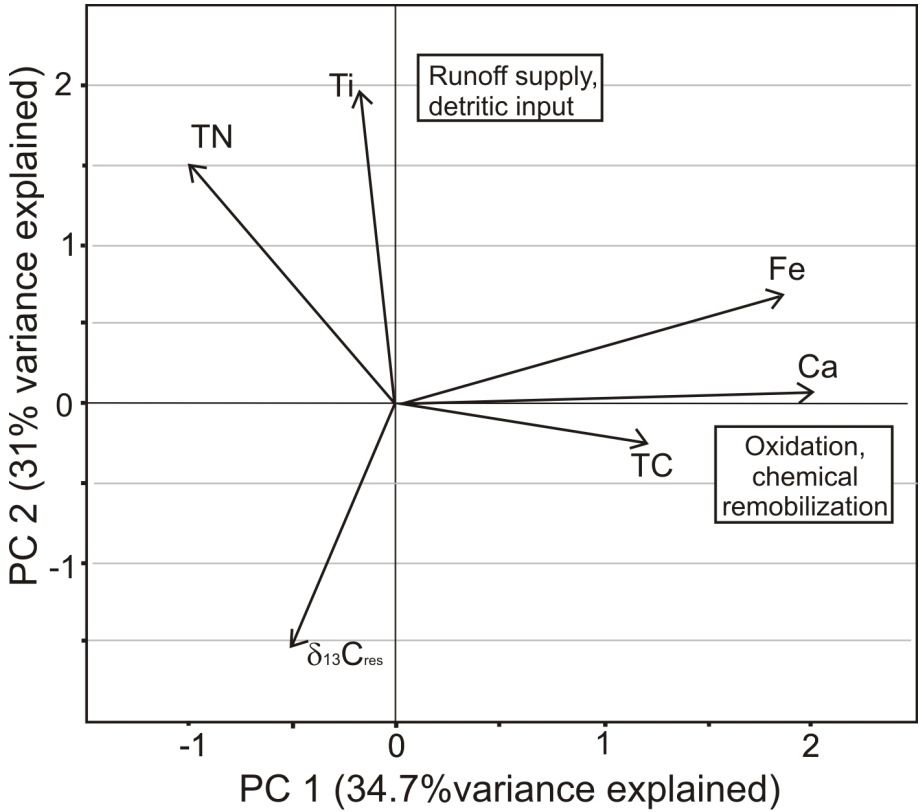

Figure 4. Principal component analysis of the geochemical data ($\delta^{13}C_{res}$ Ti, Fe, Ca, TN, TC and C/N). Two principal component axes explain more than 60 % of the variability (Axis 1: 34.7 %, Axis 2: 30.6 %). Variable loadings and sample scores are presented in the plane defined by the first two axes. Wet events are associated with high Ti and TN and with low $\delta^{13}C_{res}$, which are representative of flood conditions.

CPD
11, 1407–1435, 2015

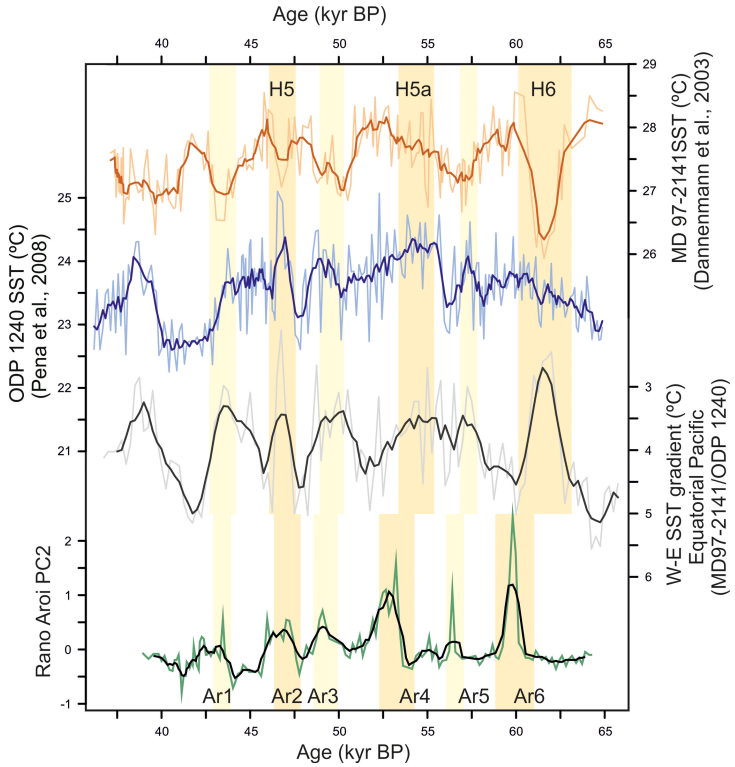

Figure 5. Comparison between Rano Aroi PC2 humidity index (green line) and W–E temperature (˚C) gradient over the Equatorial Pacific and the corresponding 5 point running average (thick black and line). The E–W gradient was obtained from the difference between MD97-2141-SST (red line, Dannenmann et al., 2003) and ODP 1240-SST (blue line, Pena et al., 2008). Wetter events in the Rano Aroi record coincide with a lower E–W temperature gradient, which implies that a displacement of the ITCZ and the SPCZ is associated with weaker oceanic circulation over the Equatorial Pacific, resembling an El Niño-like state.

CPD
11, 1407–1435, 2015

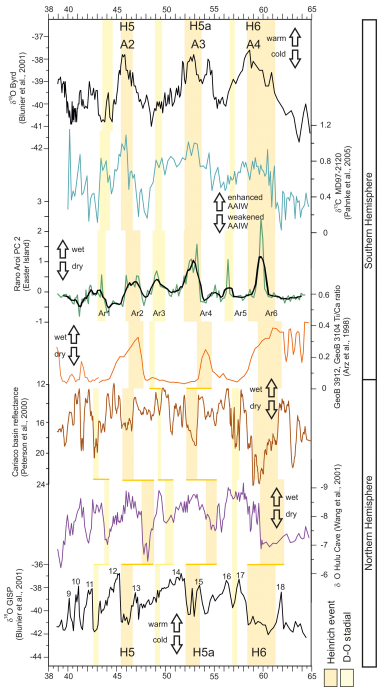

Figure 6. Records of marine sediment cores from the Cariaco Basin (ODP 1002C, Peterson et al., 2000), Sulu Sea (MD97 21–41, Dannenmann et al., 2003; Oppo et al., 2003; Rosenthal et al., 2003), South Pacific (MD97 21–20, Pahnke and Zahn, 2005) and Atlantic Caribbean (GeoB3912, GeoB3104; Arz et al., 1998); and the ice core datasets of NorthGRIP (Svensson et al., 2008) and of Byrd (Blunier and Brooks, 2001). The data presented and the correlations between each dataset have been reproduced from their original publications. North Atlantic temperature variability during DO oscillations is correlated with low-latitude millennial changes in precipitation. Northern Hemisphere records indicate the occurrence of dry periods during Heinrich stadials and other stadials and during Southern Hemisphere wet events.

CPD
11, 1407–1435, 2015